

Calibration and Validation of Numerical Models through Experimental Tests

MUHAMMAD TAYYAB NAQASH¹, GIUSEPPE BRANDO², GIANFRANCO DE MATTEIS²

¹Department of Civil Engineering, IQRA National University, Khyber Pakhtunkhawa, Pakistan

²Department of Engineering and Geology, University "G. d'Annunzio" of Chieti-Pescara, Italy

Email: engr.tayyabnaqash@gmail.com

Abstract: Finite Element Method (FEM) is an affective numerical technique oftenly used for solving models in differential form. For detailed study of any experimental test it is useful to develop a finite element model that aids in simulating the result of the experimental test precisely. This research paper is aimed at calibration and validation of an accurate numerical model. Initially, the models are suitably calibrated on the basis of experimental tests conducted by De Matteis et al [1, 2] for aluminium T-stub connections. In addition, these numerical models are also calibrated and consequently validated for the steel material using the experimental tests of Bursi and Jaspart [3, 4]. Furthermore, this paper also highlights sensitivity analysis for mesh size of different component of metal connections and different contact interations with several friction coefficients. With the help of force-displacement curves intereting results showing the accuracy of the model are provided. It is believed that the paper will help the researchers who are involved in the calibration of numerical models for metallic structures.

Keywords: T-stub connections, Finite Element Model, Calibration, Sensitivity analysis, Validation

1. Introduction:

Moment resisting frames (MRFs) are anticipated to achieve ductility through yielding in beam-column assemblies when dissipation is allowed in the connection. In this context, bolted connections are preferred on welded ones and hence widely used in such structures. Also their extensive use is due to their simplicity and economy associated during fabrication and erection phases. If bolted beam-to-column connection has to transfer moment, numerous components are involved and therefore the design calculations can be simplified if it is investigated component by component [5].

Likewise, in order to simplify the design of moment connections, modern building codes suggest the use of component method in which the concept of T-stub is in vogue as it delivers decent predictions of the parameters involved in a connection, subject to monotonic loading. The paramount role of T-stub in the component method formulation for defining strength and stiffness of joints is of prime importance. The so-called T-stub consists of two T-section elements whose flanges are symmetrically connected to each other by one or more series of bolt rows, which undergo flexural deformations due to a pulling force "P" usually transmitted by webs transversally located at the centre of the

flanges as shown in below figure:

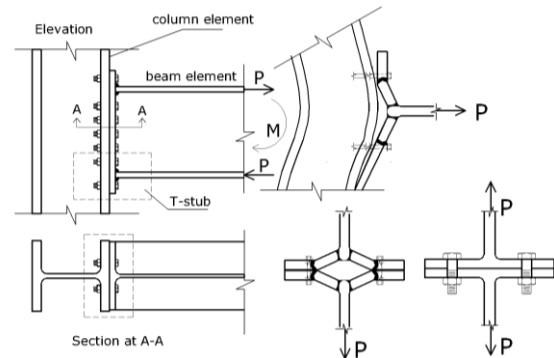


Figure 1: Idealization and schematization of T-stub

The response of the T-stub connection is to the induced internal actions depend on various phenomena, i.e., the strength and deformability of bolts, the flexural stiffness of the flange, the geometrical properties which entail different yield lines on the connected plates when incipient collapse phenomena involve the whole system, etc [6, 7].

As the Finite Element Method (FEM) is a widely used method, oftenly help in finding solution models that involve differential form and therefore in ordet to carry out detailed study of any experimental activity it is prescribed to generate a finite element model for simulating the obtained results.

2. Sensitivity analysis and numerical model for aluminium:

The base model is calibrated on the basis of available experimental tests carried out by De Matteis et al. [1] where, three welded coupons, subjected to a monotonic pulling force up to the failure, are considered. These are hereafter named as specimen “*Sample A*”, specimen “*Sample B*” and specimen “*Sample C*” [8].

The mechanical and geometrical features of tested specimens are mentioned below in Table 1, whereas the stress-strain relationship of the related materials, including also the heat affected zone closed to the welds, is provided in the forthcoming section (see Figure 3). It is important to underline that only one material, namely Aluminium alloy AW-6082, is taken into account for the T-stub flanges, keeping in one of the two T-sections so to simulate the presence of the other part of the specimen. This compels half-bolt modelling with the middle plane of the shank restrained to the end of the base body.

While considering the reduction in the diameter of the bolts due to the threaded portion, a 20% reduced area with respect to the nominal is taken into account. Generally Codes suggest a reduction of almost 25%, but in the proposed model a slightly higher resistant area of bolts is considered as the threaded portion is assumed to contribute to the stiffness. This is why a 9 mm diameter bolts instead of the nominal one (10 mm) are used for all the models in the modelling of T stub.

Meshing is used to disintegrate a physical domain (2D or 3D flats), into a simpler sub domain (element). To obtain regular mesh for bodies of irregular shape or regular bodies with holes, partitioning is require. In the FEA of metals, many mesh elements are usually deformed severely in the later stage of the

view that the developed analysis does not analyse the material hardening effect.

In order to foresee the behaviour of T-stub connections, it shall be kept in mind that they are fairly complex to model; in fact, generally their geometry is three-dimensional, material and geometrical nonlinearities are incorporated in the loading process and numerous contact phenomena, due to the interaction between flanges and bolts, are present. Hence, compromises in the modelling phase are usually considered to circumvent the mentioned difficulties.

In order to reduce the cumbersomeness of the analysis, the proposed geometry of the model (see Figure 2.a) takes into account the T-stub symmetry. As a consequence, a rigid body fixed in the space is put below the flange of analysis because they incorporate error into the analysis results and, in the worst case inverted elements can lead the analysis to terminate permanently. Hex dominant meshing is used in practice to obtain meshes including hexahedra, pyramids and tetrahedral types. As the name implies, the masher try to generate as many hexahedra as possible. The T-stub model presented over here is implemented by the Code ABAQUS 6.7 [9], where 8 node linear brick elements with reduced integration and hourglass control (*C3D8R*) are used (see Figure 2.b) for webs and flanges. The bolts are meshed with 4 node linear tetrahedron (*C3D4*) elements (see Figure 2.b). This is due to high degree of complexity in their geometry, requiring tetrahedral elements to realize a less refined mesh without jeopardizing the accuracy of the model by contact problems. Hex dominant meshing algorithm helps in obtaining meshes with a mix of hexahedral, pyramids and tetrahedral finite elements.

Table 1: T-stub tested specimens used for calibration of the proposed models

Sample ID	Aluminium Alloy for flange	Aluminium Alloy for web	Bolt Material	Flange Thickness [mm]	Web Thickness [mm]	Bolt Diameter [mm]
Sample A	6082	7020	4.8	10	12	10
Sample B	6082	7020	7075	10	12	10
Sample C	6082	7020	10.9	10	12	10

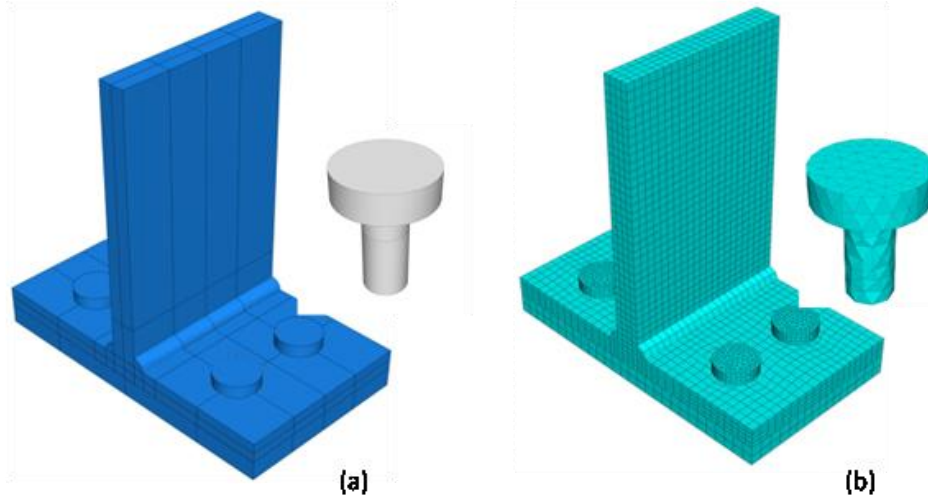


Figure 2: T-stub, (a) Geometry and (b) FEM model

The T-stub web in consideration is pulled when a uniform vertical displacement Δ is applied to a reference point constrained by a rigid coupling with the top of the web itself. Whereas, the bottom part of the rigid body below the T-stub flange is deemed to be fixed by applying a clamping boundary condition.

In order to consider application of bolt loading, tool exists in Abaqus/CAE, and therefore is used for the application of bolt load, with proper amplitude. In general, the process of defining the bolt loading requires multiple steps that span multiple modules, therefore bolt load is defined in the first step using static general analysis and are subjected to the preload force acquire from Equation (1).

$$F_{p,Cd} = 0.7 \times f_{ub} \times A_s \quad (1)$$

Where A_s is the resisting area of the bolt and f_{ub} is the ultimate stress of the bolt material.

In a finite element analysis, contact conditions are treated as special class of discontinuous constraint, allowing forces to be transmitted. The constraint is discontinuous within the domain of the model because it is applied when and only the two surfaces interact and if on the contrary these surfaces separate, no constraint is applied. The analysis must be able to detect about when two surfaces are in contact and apply the contact constraints accordingly. Similarly, it shall detect when two surfaces separate and remove the contact constraints. Surfaces are defined from the element faces of the underlying material. Three contact interactions are defined, namely *i*) the bearing of the back of the T-stub section against the interface with the rigid body, *ii*) the interaction between the hole and the bolt shank and *iii*) the

interaction between the bolts head and the surface of the T-stub. The first is defined as a penalty contact (characterized by a friction coefficient of 0.3) and the later two as frictionless contact.

The material constants used for all Aluminium parts are $E=70,000$ MPa (elastic modulus), $\nu = 0.3$ (Poisson's ratio) and $\rho = 2700$ kg/m³ (material density), whereas steel bolts are modelled with $E = 210,000$ MPa, $\nu = 0.3$ and $\rho = 7600$ kg/m³. The proof strengths for all the aluminium components of the T-stub are referred to a conventional stress of $f_{0.2}$.

While defining plasticity data in Abaqus, use of true stress/strain is immensely of vital importance. Abaqus requires these values to interpret the data correctly. The material test data are supplied using values of nominal stress and strain. Quite oftenly to convert the plastic material data from nominal stress/strain values to true stress/strain values it is therefore required. The relationship between true stress/strain and nominal stress/strain is described in eq. (2).

$$\sigma = \sigma_{nom} \times (1 + \epsilon_{nom}) \quad \text{eq. (2)}$$

The classical metal plasticity model in Abaqus defines the post-yield behavior for most metals. Abaqus approximates the smooth stress-strain behavior of the material with a series of straight lines joining the given data points. Any number of points can be used to approximate the actual material behavior, therefore, to use a very close approximation of the actual material behaviour making it possible. The plastic data defines the true yield stress of the material as a function of true plastic strain. The first piece of data given

defines the initial yield stress of the material and, therefore, should have a plastic strain value of zero. Instead, there will probably be the total strains in the material. Therefore these total strain values are decomposed into the elastic and

$$\epsilon_{pl} = \left[\ln(1 + \epsilon_{nom}) - \frac{\sigma_{nom}}{E} \right] \text{eq. (3)}$$

where, σ_{true} and ϵ_{pl} are the true stress and plastic strain respectively, σ_{nom} and ϵ_{nom} are the nominal stress and strain respectively, and E is the Elastic Modulus.

In order to interpret correctly the behaviour of the system (also for large deformation), the available material test data [16, 17] are properly transformed in true stress-true strain, as depicted in Figure 3, where the experimental curves are also provided for all the tested specimens.

The analysis of the models is accomplished by standard multiple step (two steps) analysis. In the first step, the bolt preload is applied statically by means of the “*bolt load*” option,

plastic strain components. The plastic strain is obtained by subtracting the elastic strain defined as the value of true stress divided by the Young’s modulus from the value of total strain as mentioned in eq. (3).

provided in the ABAQUS library. In the second step, a static Riks analysis is applied till the whole system collapsed in order to reproduce the loading process of the whole T-stub.

A preliminary sensitivity analysis is carried out on specimen Sample A, to see the influence of mesh size, finite element adoptions and contact typology on the proposed model response. To this purpose, in the first stage, T-stub models with approximate global mesh sizes of 3mm, 4mm and 5mm (see Figure 4.a, Figure 4.b and Figure 4.c, respectively) are analysed. The obtained number of elements, as well as the corresponding CPU time consuming are enlisted in Table 2.

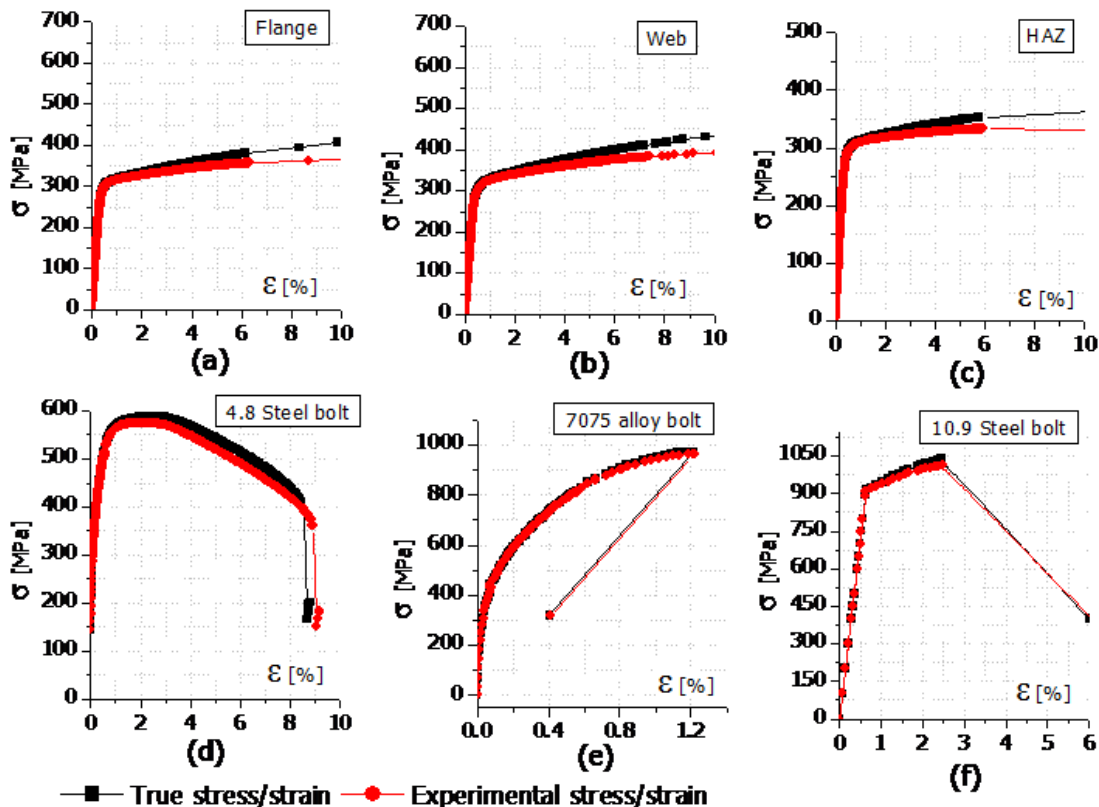


Figure 3: Experimental and true stress/strain curves for: (a) Flange, (b) Web, (c) HAZ, (d) 4.8 steel bolts, (e) 7075 aluminium bolts and (f) 10.9 steel bolts

Table 2: Mesh size of T-stub model, related number of elements and nodes

Approximate global mesh size	No. of nodes	No. of elements [C3D8R]	CPU time [sec]
3mm	12738	9700	4453
4mm	8412	6344	3876
5mm	4271	2976	1450

After analysing the obtained response, given in Figure 6.a in terms of pulling force F vs. vertical displacement Δ , that the selected mesh sizes does not influence significantly can be observed the overall result. However, since using a global mesh size of 4mm requires sustainable time analysis consuming, giving precisely the same results of a 3mm mesh side length, hence the former is assumed and suggested for the models to be used in any parametric study.

The same type of remarks are said to be valid for finite elements typology and size of bolts. With respect to the options listed in Table 3, it can be observed observe that using C3D4 elements with an average mesh size of 3mm gives the same results of C3D8R elements with 1mm mesh side

length, requiring half of the CPU time. And, the former mesh typology is adopted for this very reason (see Figure 5.b).

Finally, the sensitivity of the model with respect to the four different contacts combination listed in Table 4 is investigated. All the possible combinations need an equivalent CPU time, yielding as a result approximately the same outcomes for smaller displacements. Nevertheless, contacts “combination 1”, with penalty coefficient of 0.3 for the “*T-stub to base*” and frictionless contacts for “*bolt to T-stub*”, is assumed as it gives comparatively lesser convergence problems in case of larger displacements.

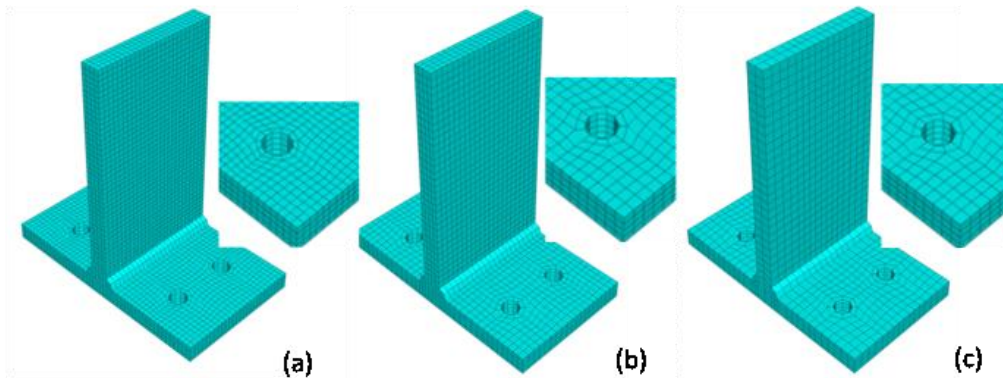


Figure 4: Sensitivity analysis for mesh size (a) 3mm, (b) 4mm, and (c) 5mm

Table 3: Mesh size for bolt model, related number of elements and nodes

Approximate global mesh size	Element type	No. of nodes	No. of elements	CPU time [sec]
1mm	C3D4	3136	13336	8202
2mm	C3D4	612	2303	5700
3mm	C3D4	249	860	3876
4mm	C3D4	166	525	2124
3mm	C3D8R	372	248	947
1mm	C3D8R	5595	4664	6681

Table 4: Different contact combinations

Combination	T-stub to base	T-stub to bolts	CPU time [sec]
1	Penalty-0.3	Frictionless	3876
2	Penalty-0.3	Rough	3698
3	Penalty-0.1	Frictionless	3359
4	Penalty-0.2	Frictionless	2884

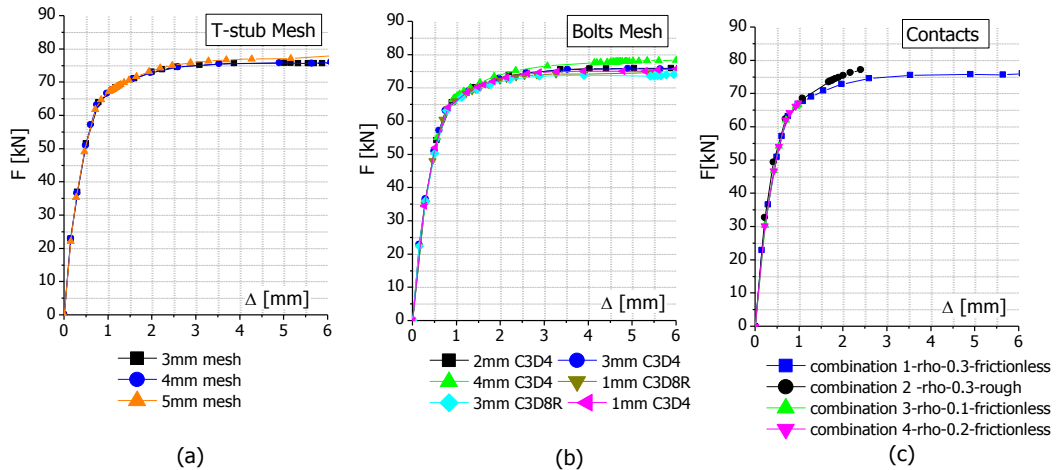


Figure 5: Sensitivity analysis for: (a) T-stub mesh, (b) Bolts mesh, and (c) Contacts

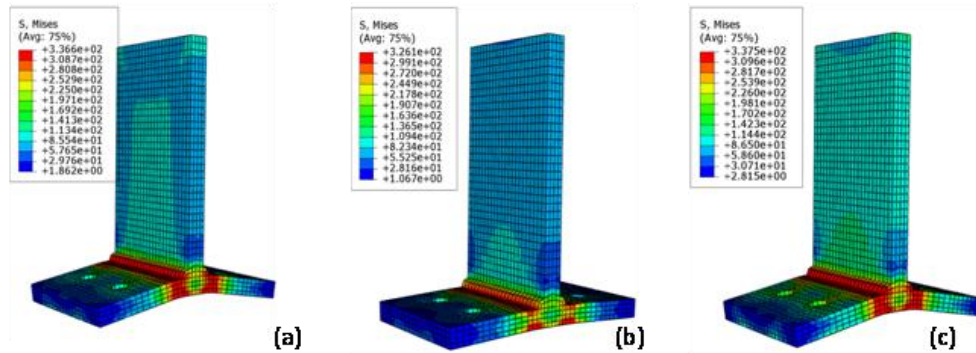


Figure 6: Deformed shapes and stress contour of (a) FEM specimen A, (b) FEM specimen B and (c) FEM specimen C

The reliability of the proposed aluminium T-stub models can be verified by comparing the experimental outcomes with the numerical ones. As shown in Figure 6.a, in case of experimental specimen Sample A, a failure “mode 2a” is detected, whereas for specimens “Sample B” and “Sample C” failure modes 2b and 1 are

observed, respectively. The same failure modes occurs in case of numerical model (Figure 6). On the other hand, the proposed numerical results are in decent agreement with the experimental ones, if compared in terms of Force vs. Displacement curves (Figure 7).

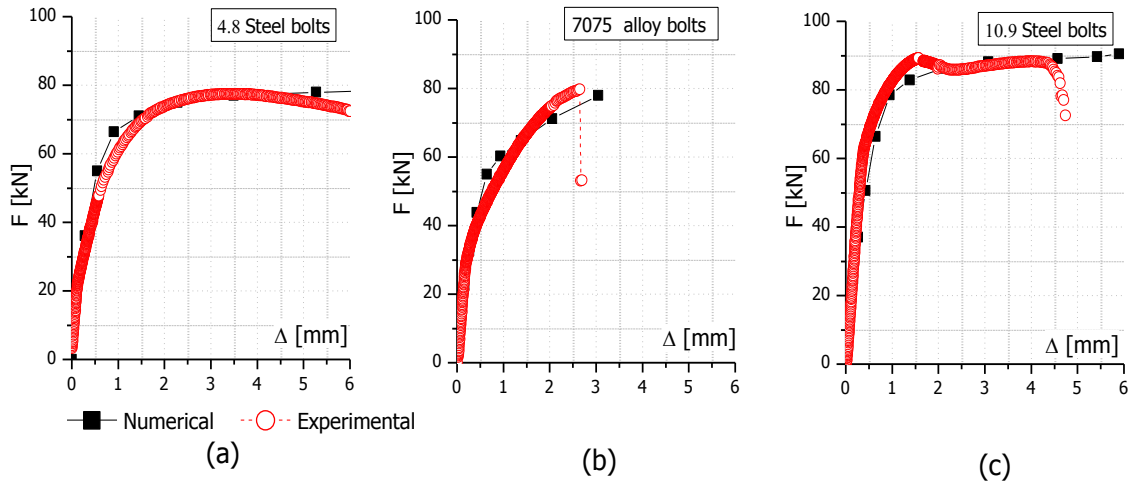


Figure 7: Experimental vs numerical results for: (a) 4.8 steel bolts, (b) 7075 aluminium bolts, and (c) 10.9 steel bolts

3. Description and calibration of the steel model

The previous model which is calibrated for the Aluminium material is now checked using steel material on the basis of experimental tests carried out by Bursi and Jaspart [3, 4] (see Figure 8). In particular, two specimens are taken into account with preloaded and non-preloaded bolts; and both these specimens are subjected to a monotonic pulling force up to the failure. These specimens are hereafter named as “Sample PL1”, “Sample NPL1”, “Sample PL2” and “Sample NPL2”. The mechanical and geometrical features of tested specimens by Bursi and Jaspart are provided in Table 5.

In these models, for reducing the cumbersomeness in the analysis the proposed geometry of the model takes into account the T-stub symmetry initially (see Figure 10). Nevertheless, in order to validate the calibration process a complete back to back model is developed during the calibration process as shown in

Figure 9. In the symmetrical model, a rigid body fixed in the space is put below the flange of one of the two T-sections so to simulate the presence of the other part of specimen. For the same reason, only half of the bolts are modelled, with the middle plane of the shank restrained with the end of the base body [10].

Table 5: Specimens with material properties of tested T-stub connections (Bursi and Jaspart)

Sample ID	Profile	8.8 Grade steel Bolts		Flange material		Web material		Bolt ϕ (mm)
		f_y (MPa)	f_u (MPa)	f_y (MPa)	f_u (MPa)	f_y (MPa)	f_u (MPa)	
PL1	IPE300	800	1031	390	772	430	772	12
NPL1	IPE300	800	1031	390	772	430	772	12
PL2	HEB220	740	964	260	651	260	664	12
NPL2	HEB220	740	964	260	651	260	664	12

Likewise for Aluminium, the T-stub model is implemented by the Code ABAQUS 6.7 [9], where 8 node linear brick elements with reduced integration and hourglass control (C3D8R) are used for webs and flanges. Similarly, bolts are meshed with 4 node linear tetrahedron (C3D4) elements (see Figure 9 and 10). In the calibration process of the back to back T-

stub model, the T-stub is pulled through its web by imposing a uniform vertical displacement (Δ), applied at a reference point which is constrained by a rigid coupling with the top of the web surface, whereas, the bottom T-stub is fixed in space by a clamping boundary condition.

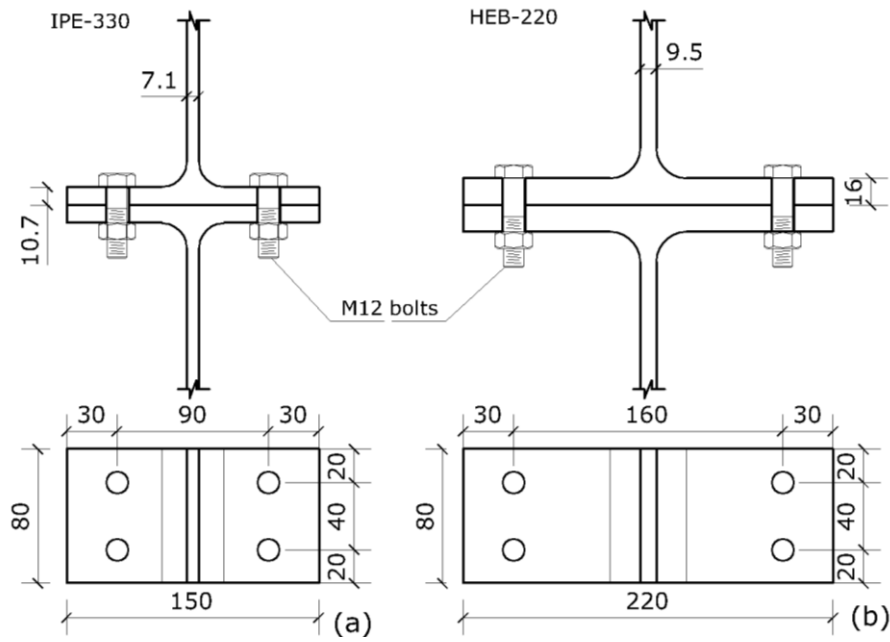


Figure 8: Geometrical characteristics of tested T stub specimens:(a) IPE300 (b) HEB-220

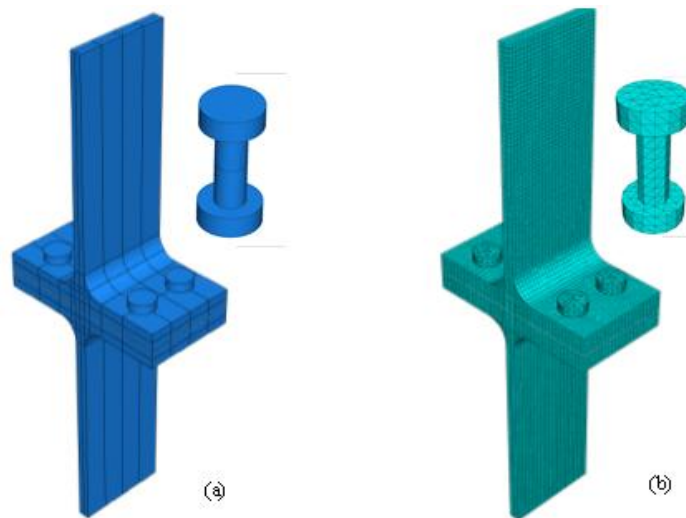


Figure 9: T-stub model with complete assembly for calibration and validation process: (a) Geometry and (b) FEM

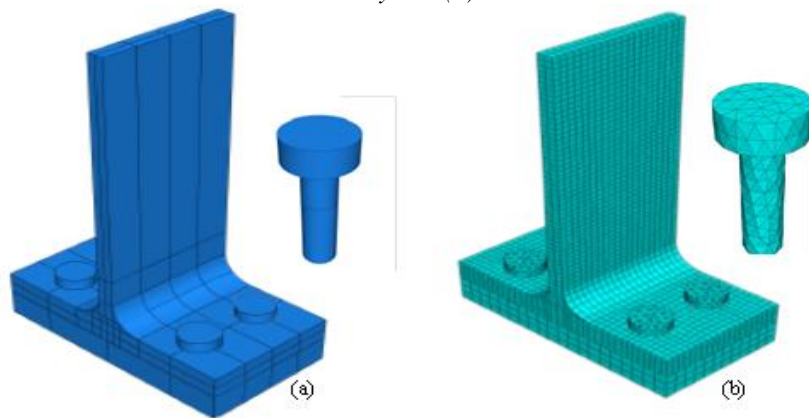


Figure 10: T-stub model with symmetry for calibration process to be used in parametric analysis: (a) Geometry and (b) FEM model

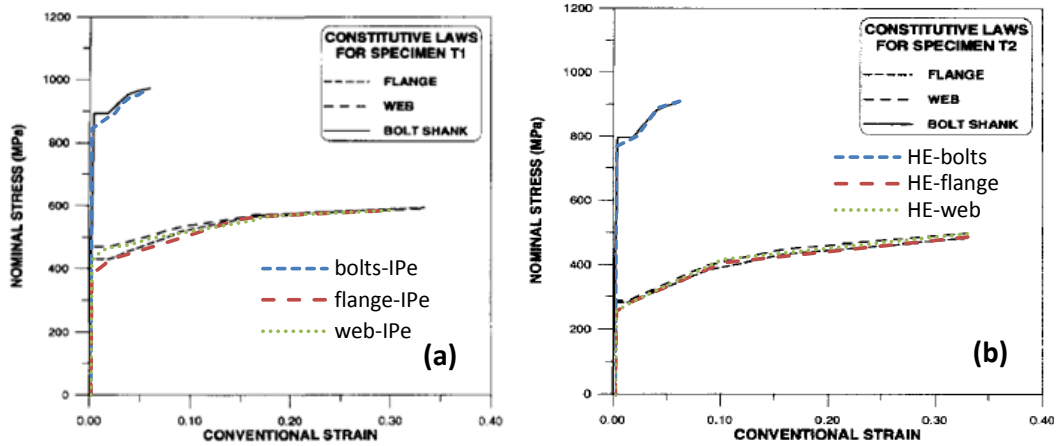


Figure 11: Material adopted for models used in calibration process according to Bursi and Jaspart experimental tests:(a) IPE-300 and (b) HEB-220

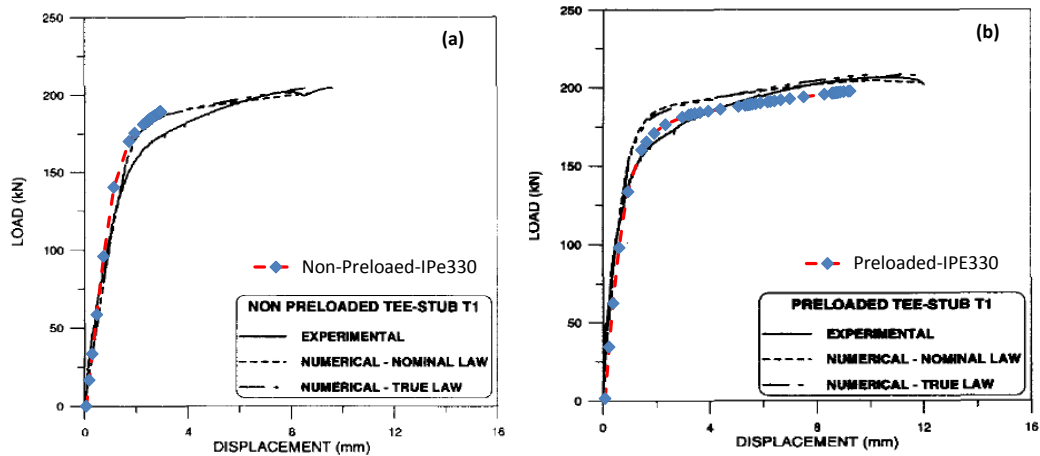


Figure 12: Numerical versus experimental-and-numerical results of Bursi and Jaspart for: (a) NON-preloaded IPE-300 model (NPL1) and (b) for preloaded IPE-300 model (PL1)

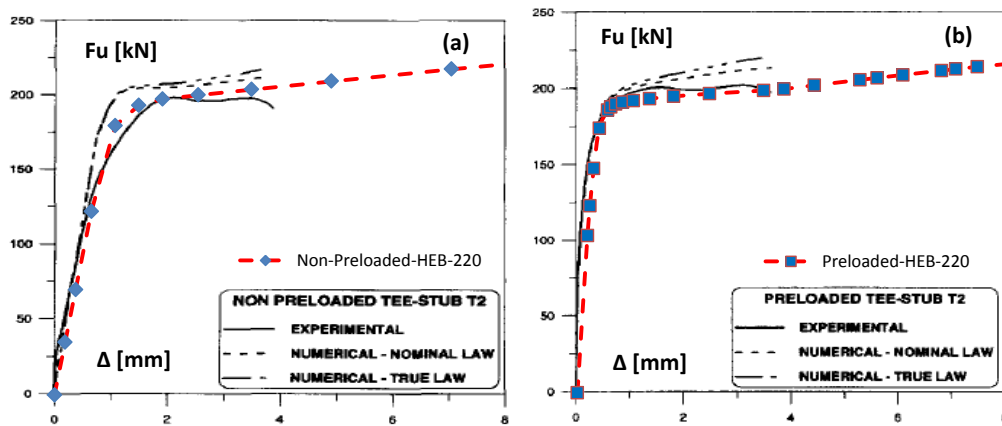


Figure 13: Numerical versus experimental-and-numerical results of Bursi and Jaspart for: (a) NON-preloaded HE-220 model (NPL2) and (b) for preloaded HE-220 model (PL2)

The material constants used for all parts are $E=210000\text{N/mm}^2$ (Elastic modulus), $\nu=0.3$ (Poisson's ratio) and $\rho=7600\text{kg/m}^3$ (Material density). The material adopted for the specimens in the calibration phase are shown in Figure 11. The reliability of the proposed models is thus proved by comparing the experimental and numerical outcomes. As a results, the models are

proved reliable (see Figure 12, for specimens PL1 and NPL1 and Figure 13, for specimens PL2 and NPL2). In order to validate the assumption for considering the symmetry of the system two different types of models are calibrated. The results are shown only for the symmetrical model as it is considered in the parametric analyses. It is also interesting to note

that Bursi and Jaspart experimental curves are associated with complete models inspite of the results, obtained in our case, when symmetry is taken into account [11].

Conclusions:

The paper initially deals with the calibration of T stub models for Aluminium materials. These models are then checked using steel materials aiming to validate the assumed models. In case of Aluminium, a complete sensitivity analysis has been conducted where the influence of contact interaction, mesh size of T stub as well as several mesh size of bolts are considered, thus providing useful information for researchers who are involved in the simulation of such systems. The effect of preload using two step analysis is also considered in the calibration of Aluminium T stubs which shows that it is important to take it into consideration. The numerical models are calibrated for Aluminium by comparing the failure mechanisms as well as by plotting the force-deformation curves obtained from numerical models with those of the experimental study of De Matteis et al. After the calibration of the numerical model for Aluminium T stubs, the same model has been considered using steel material. In this case, the model is in good agreement with the experimental results of Bursi and Jaspart. These models are validated for complete geometry. It can be summarized that such numerical models are believed to be accurate for obtaining the real behaviour of the systems and therefore it is suggested for the researchers as well as technicians involved in such type of modelling.

References:

- [1] De Matteis, G., Brescia, M., Formisano, A., Mazzolani, F.M., *Behaviour of welded aluminium T-stub joints under monotonic loading*. Computers & Structures, 2009. **87**(15-16): p. 990-1002.
- [2] De Matteis, G. and F.M. Mazzolani. *Behaviour of Welded Aluminium T-Stub Connections: Experimental Analysis and Interpretative Models*. 2006: ASCE.
- [3] Bursi, O. and J.-P. Jaspart, *Calibration of a finite element model for isolated bolted end-plate steel connections*. Journal of Constructional Steel Research, 1997. **44**(3): p. 225-262.
- [4] Bursi, O. and J.-P. Jaspart, *Benchmarks for finite element modelling of bolted steel connections*. Journal of Constructional Steel Research, 1997. **43**(1): p. 17-42.
- [5] Naqash, M.T., G. De Matteis, and A. De Luca, *Seismic design of Steel Moment Resisting frames-European Versus American Practice*. NED University Journal of Research, 2012. **Thematic Issue on Earthquake**: p. 45-59.
- [6] De Matteis, G., M.T. Naqash, and G. Brando. *Parametric Analysis of Welded Aluminium T-Stub Connections*. in *Proceedings of the Thirteenth International Conference on Civil, Structural and Environmental Engineering Computing*. 2011: Civil-Comp Press, Stirlingshire, UK,.
- [7] Swanson, J.A. and R.T. Leon, *Bolted steel connections: Tests on T-stub components*. Journal of Structural Engineering, 2000. **126**(1): p. 50-56.
- [8] De Matteis, G., M.T. Naqash, and G. Brando. *Aluminium T-stub connections: additional parametric analysis for the evaluation of effective width*. in *XXIII Italian steel conference (CTA 2011)*. 2011. Lacco Ameno, Ischia, Naples.
- [9] Hibbit, D., B. Karlsson, and P. Sorenson, *ABAQUS reference manual 6.7*. 2005, Pawtucket: ABAQUS Inc.
- [10] Naqash, M.T., G. Brando, and G. De Matteis. *On the effective length of metal T-stub connections with thick flanges*. in *XXIV CTA Italian steel conference*. 2013. Torino, Italy.
- [11] De Matteis, G., M.T. Naqash, and G. Brando, *Effective length of aluminium T-stub connections by parametric analysis*. Engineering Structures, 2012. **41**: p. 548-561.